Renewable Energy 145 (2020) 2159–2168

Contents lists available at ScienceDirect

Renewable Energy

journal homepage: www.elsevier.com/locate/renene

Kinetic study of the pyrolysis of microalgae under nitrogen and CO_2 atmosphere

Yu Hong [a, d], Chengrui Xie [a], Wanru Chen [a], Xiang Luo [a, b], Kaiqi Shi [a, b], Tao Wu [b, c, *]

[a] Department of Chemical and Environmental Engineering, The University of Nottingham Ningbo China, Ningbo, 315100, China
[b] New Materials Institute, The University of Nottingham Ningbo China, Ningbo 315100, China
[c] Municipal Key Laboratory of Clean Energy Conversion Technologies, The University of Nottingham Ningbo China, Ningbo 315100, China
[d] Research and Development Centre, Ningbo Thermal Power Co. Ltd., Ningbo, 315040, China

ARTICLE INFO

Article history:
Received 21 April 2019
Received in revised form
29 June 2019
Accepted 29 July 2019
Available online 30 July 2019

Keywords:
Kinetics
Pyrolysis
Algae
Model compound
Carbon dioxide

ABSTRACT

In this study, three primary components of algae (lipid, carbohydrate and protein) and one microalgae (spirulina) were pyrolyzed using a thermogravimetric analyser (TGA) under nitrogen and CO_2 atmosphere at four heating rates. It was found that protein decomposed first, followed by carbohydrate and then lipid. The kinetic study revealed that the lowest activation energy for the initiation of the pyrolysis of ovalbumin (protein) is ~70 kJ/mol. Oil droplet showed higher activation energy of 266.5 kJ/mol during its pyrolysis in the CO_2 atmosphere, which suggests that algal lipid is more difficult to decompose in the CO_2 atmosphere. However, for the pyrolysis of cellulose (carbohydrate), the activation energy (~310 kJ/mol) is similar under two different gas atmospheres tested. This study showed that CO_2 atmosphere favors the pyrolysis of algae with high protein content and low lipid content, since the existence of CO_2 promotes the cracking of VOCs (volatile organic compounds) as well as the reaction between VOCs and CO_2.

1. Introduction

As a renewable carbonaceous resource, marine biomass has attracted special interests as a fuel source and is regarded as a potential substituent to traditional fuels. The terrestrial biomass is primarily comprised of cellulose, hemicellulose and lignin [1], while algal biomass consists of carbohydrates, proteins, and lipids, which has been investigated by many researchers on its conversion to various biofuels [2–6].

Thermogravimetric analysis (TGA) is commonly used to study the thermal decomposition of algae and its model components. Numerous research has been focused on the thermal degradation of biomass based on the weight change against temperature [7–9]. Two commonly-used iso-conversional methods, i.e. Kissinger-Akahria-Sunose (KAS) and Flynn-Wall-Ozawa (FWO), were applied to study the kinetics of pyrolysis and thus to determine kinetic parameters such as activation energy (E_a) and pre-exponential factor (A) [8,10,11]. However, the decomposition of different components in biomass leads to extremely complicated pyrolysis processes, which make the iso-conversional method inappropriate to reveal the nature of the processes [12]. Recently, the model fitting method has been adopted to simulate the kinetics of biomass pyrolysis by substituting different reaction models into the Coats-Redfern function. The highest regression value of such indicates the best mechanism model for the description of the pyrolysis of biomass [13].

The conventional pyrolysis of biomass and the kinetic study have been discussed in many previous studies [8,10,12,14–16]. It is reported that compared with N_2, the use of CO_2 as the carrier gas could assist the pyrolysis of carbonaceous materials and lead to benefits such as higher thermal efficiency, reduced tar formation, higher production of syngas (especially CO) [17,18]. However, there is not much work that has been carried out on the kinetics of the pyrolysis of algal model compounds under CO_2 atmosphere, as well as the comparison of the pyrolysis of algae under two different atmospheres, i.e., CO_2 atmosphere and N_2 atmosphere.

In this study, a kinetic study of the pyrolysis of three model compounds, i.e., carbohydrate, lipid and protein, and spirulina (microalgae) under N_2 and CO_2 atmospheres was conducted. Iso-conversional method (Kissinger- Akahira-Sunose method) and

* Corresponding author. New Materials Institute, The University of Nottingham Ningbo China, Ningbo 315100, China.
E-mail address: tao.wu@nottingham.ac.uk (T. Wu).

https://doi.org/10.1016/j.renene.2019.07.135
0960-1481/

model fitting method (Coats-Redfern method) were applied to derive the activation energy (E_a) and pre-exponential factor (A). Elemental compositions of char obtained under N_2 and CO_2 atmosphere were derived by using SEM-EDS (Scanning Electron Microscope-Energy Dispersive Spectrometer) and compared to reveal the pyrolysis of algae.

2. Materials and methods

2.1. Materials

Oil droplet (Optima 339 powdered vegetable fat), α- Cellulose ($(C_6H_{10}O_5)_n$, Aladdin®, product code C104844) and ovalbumins (Sinopharm Chemical Reagent Co., Ltd, product code 69003835) were selected to represent and simulate the pyrolysis of lipid, carbohydrate, protein contents in algae, respectively, following the approach used by other researchers [19–21]. Spirulina, the algae sample, was provided by Shandong Binzhou Tianjian Biotechnology Co. Ltd. (Shandong Province, China). Raw materials were milled (Retsch ZM200 Ultra-Centrifugal mill) and sieved to the same particle size of smaller than 120 μm.

2.2. Characterization of algae primary model compounds

The results of proximate, elemental and composition analyses are listed in Table 1, the procedure can be found in our previous studies [22–25]. The composition of protein, lipid and carbohydrate in biomass was determined by Kjeldahl method (BS EN ISO 20483:2013), Soxhlet extraction method (GB/T 5009.6–2003), and the difference calculated (GB/Z 21922–2008), respectively.

2.3. Kinetic analysis method

Pyrolysis of the three algal pseudo-components and spirulina via conventional electric heating method was conducted on a thermogravimetric analyser (TGA, NETZSCH STA449F3, Germany) using non-isothermal process. Four different heating rates, i.e., 5, 10, 20 and 50 °C/min, were used to heat the samples from 50 to 900 °C. The weight loss profile of each sample was subsequently derived. Pure nitrogen or carbon dioxide with a flowrate of 20 mL/min was introduced into the system as the carrier gas and to provide an oxygen-free atmosphere. The initial sample weight for each experiment was 2 ± 0.5 mg. All experiments were repeated at least once to ensure accuracy and repeatability.

In order to investigate the effects of CO_2 on the carbon contained in solid residue, char samples were first prepared in a tube furnace (SG-GL1200K, Shanghai) using the same TGA heating programme, i.e. all samples were heated from 50 to 900 °C with a heating rate of 5 °C/min under a N_2 purge of 20 mL/min. The char samples collected were then analysed using a TGA in CO_2 following the procedure described previously.

Table 1
Characteristics of cellulose, ovalbumin, oil droplet and spirulina.

	Ovalbumin	Cellulose	Oil droplet	Spirulina
Proximate analysis (wet basis, wt. %)				
Moisture content	2.0	2.7	0	6.7
Volatile matters	86.6	88.6	100.0	73.5
Fixed carbon	9.9	7.6	0	13.2
Ash content	0	1.1	0	6.6
Ultimate analysis (dry ash free basis, wt. %)				
C	41.6	42.7	75.8	49.8
H	7.0	6.5	11.8	6.6
N	12.2	0	0	11.0
S	1.2	0	0	0.7
O	38.0	50.8	12.4	31.9
HHV (MJ/kg)	18.73	16.99	39.07	20.55
Composition of sample (wt. %)				
Protein	81.6	0	0	57.8
Lipid	1.1	1.2	99.6	2.9
Carbohydrate	7.9	97.1	0.1	23.4

2.3.1. Determination of kinetic parameters

Thermal decomposition of algae is a typical solid decomposition reaction, the rate of which is defined as,

$$\alpha = \frac{m_0 - m_T}{m_0 - m_f} \quad \text{Eq. (1)}$$

Where m_0 is the initial mass of the material, m_f is the final mass of the solid material after pyrolysis, m_T is the mass of material at reaction temperature of T.

The kinetic study is based on the Arrhenius Law. According to Eq. (1), the conversion rate only depends on the reaction temperature. The thermal dynamic formula can be described as following,

$$\frac{d\alpha}{f(\alpha)} = \frac{A}{\beta}\exp\left(\frac{-E_a}{RT}\right)dT \quad \text{Eq. (2)}$$

Where $f(\alpha)$ is the conversion (α)-dependent function; $\beta = \frac{dT}{dt}$ is the heating rate, K/min; E_a is the activation energy, J/mol; A is the pre-exponential factor, min^{-1}; R is the universal gas constant, 8.314 J/mol· K; T is the absolute temperature, K.

The integration of Eq. (2) over α is expressed as,

$$G(\alpha) = \int_0^{\alpha} \frac{d\alpha}{f(\alpha)} = \frac{A}{\beta}\int_0^{T} exp\left(\frac{-E_a}{RT}\right)dT \quad \text{Eq. (3)}$$

Where $G(\alpha)$ is the integrated form of $f(\alpha)$.

2.3.2. Iso-conversional method: Kissinger- Akahira-Sunose (KAS)

Generally, the activation energy and the pre-exponential factor of one-step fluid state reactions are constant, but these parameters change with the change in conversion rate (α) for reactions involving solid, due to its internal heterogeneity of solid samples and complicated reaction mechanism [26]. Therefore, iso-conversional methods are more appropriate to be applied to determine the kinetic parameters of solid-state reactions.

KAS method is based on Arrhenius Equation using differential methods [26,27],

$$G(\alpha) = \frac{AE_a}{\beta R}p\left(\frac{E_a}{RT}\right) \quad \text{Eq. (4)}$$

Combined with Eq. (3), the variables of A, E_a and $f(\alpha)$ are related to T, while A and E_a are independent of α. Hence, Eq. (3) can be further integrated into the following form,

$$ln\frac{\beta}{T^2} = \ln\left(\frac{RA}{E_a G(\alpha)}\right) - \frac{E_a}{RT} \quad \text{Eq. (5)}$$

The plot of $ln\frac{\beta}{T^2}$ versus $-\frac{1}{RT}$ for the constant α will derive a linear relationship.

To reveal the correlation between E_a and α, 19 conversion rates from 5 to 95% were selected. The E_a can be determined by the gradient of the linear profile.

2.3.3. Model fitting method: Coats-Redfern method

The Coats-Redfern method is one of the model fitting approaches that can be used to calculate the kinetic parameters as well as to determine the order and mechanism of the reaction [28].

Coats-Redfern approximation was applied and further rearranged as,

$$ln\frac{G(\alpha)}{T^2}=\ln\left[\frac{AR}{\beta E_a}\left(1-\frac{2RT}{E_a}\right)\right]-\frac{E_a}{RT} \quad \text{Eq. (6)}$$

The function $G(\alpha)$ is dependent on the reaction model adopted [29].

The common value of $\frac{2RT}{E_a}$ is far less than 1, which can normally be disregarded. Therefore, the equation could be simplified as,

$$ln\frac{G(\alpha)}{T^2}=\ln\left(\frac{AR}{\beta E_a}\right)-\frac{E_a}{RT} \quad \text{Eq. (7)}$$

By substituting different forms of $G(\alpha)$ into Eq. (7), a plot of $ln\frac{G(\alpha)}{T^2}$ versus $-\frac{1}{RT}$ is linear with a slope equal to E_a, and the interception point provides values of E_a and A.

3. Results

3.1. Thermogravimetric analysis

Previous workers have examined single reaction model, and multiple parallel reaction model consisting up to seven-reactions based on different components or constituents in algae with different reactivity [30]. In previous study, ovalbumin [19], cellulose [20], and oil droplet [21] were used to represent protein, carbohydrate and lipid in algae, therefore, these compounds were chosen in this study to represent the protein, carbohydrate and lipid content in spirulina. The simulated TGA and DTG curves of spirulina were calculated using the sum of each TGA and DTG data of three model compounds multiplied to the corresponding composition of protein, carbohydrate, and lipid content in spirulina (Table 1). As shown in Fig. 1 and Fig. 2, the use of these three components could simulate the actual alga with relatively satisfactory accuracy, the same as what was reported by other researchers [31,32]. Multiple pyrolysis of algal model compounds, spirulina, and the calculated data for spirulina at heating rates of 5, 10, 20 and 50 °C/min are illustrated in Figs. 1 and 2 to reveal its mechanism [33]. Although the heating rates were different, the TG curves were comparable with similar initial and final temperatures. However, the peak value of DTG curve shifted to a higher temperature zone as the heating rate increased and reached the set maximum of 50 °C/min. This phenomenon is attributed to the hysteresis in heat transfer from the crucible to sample, as well as the difference in actual temperature of the samples and that of the measured temperature of the crucible. Moreover, the larger amount of volatile matter released with elevating heating rate. The comparison of DTG curves under N_2 and CO_2, ovalbumin showed higher weight loss rate under CO_2, while the rate of weight loss for oil droplet and cellulose remained unchanged.

Figs. 1 and 2 show that the degradation pattern of model compounds and algae were similar to three typical stages involving dehydration, volatilization and carbonization under both N_2 and CO_2 atmospheres. The first stage started from ambient temperature to the temperature where light volatiles began to release, during which the moisture in biomass was removed at around 105 °C. Although only slight weight loss has been observed during this stage, structure of the sample has changed. A significant weight loss was recorded in the second stage ranging from 150 to 500 °C, primarily due to the devolatilization of organic matters. Ovalbumin, cellulose, oil droplet and spirulina decomposed mainly in the temperature range of 180–250, 290–370, 330–470 and 220–400 °C, respectively. Given the low decomposition temperature, it can be inferred that the protein and carbohydrate of algae are of low thermal stability, while lipid is of high thermal stability under both atmospheres. This waste losst is regarded as the main pyrolysis stage. The third stage (500–800 °C) showed a steady weight loss, which was resulted from the decomposition of non-volatile carbonaceous residues. Char was formed while CO_2 and CO were removed [34,35].

As evident from Figs. 1 and 2, ovalbumin decomposes at lower pyrolysis temperature, followed by cellulose and oil droplet, which means proteins in algae would decompose first, then carbohydrates and lipids. The increasing heating rate raises the weight loss rate of each sample. Among the four samples, the cellulose has the highest weight loss rate, then oil droplet, at four different heating rate under both N_2 and CO_2. The TG curve of the model spirulina is relatively similar to that of the actual spirulina under both atmospheres. As for the DTG curves, the theoretical weight loss rate has two peak values, around 200 and 350 °C under both atmospheres, which is similar to the DTG curve of the pyrolysis of ovalbumin. This is due to the excessive undefined substances contained in ovalbumin, rather than in spirulina. Therefore, the first peak in DTG curves of both spirulina and its model curve is attributed to those components that are not within the scope of the model compounds. The second peak appeared at higher pyrolysis temperature (normally around 300–400 °C) with larger weight loss rate is likely associated with the thermal hysteresis.

The CO_2 gasification of carbon normally occurs more significantly at high-temperature range above 800 °C and leads to the significant consumption of carbonaceous residues [36]. Therefore, for comparison of the pyrolytic behavior under two different atmospheres, the lower temperature range of the TGA curves (100–800 °C) is examined in this study. Table 2 summarizes the primary pyrolysis parameters including Y_{char}, the weight percentage of char residue at 800 °C; T_i, the initial temperature when volatile matters start to release; D_m, the maximum weight loss rate; T_m, the peak temperature; $\Delta T_{1/2}$, the half-peak width temperature, which were all derived from TG and DTG curves (Figs. 1 and 2). From Table 2, the char residue of oil droplet, cellulose, ovalbumin and spirulina after pyrolysis remained relatively unchanged under both atmospheres for the different heating rates. Due to the thermal hysteresis, D_m, T_m and T_i increased with increasing heating rate as observed in both atmospheres. It has been previously reported that the higher heating rate could reduce the reaction time and postpone the pyrolysis [37]. Moreover, according to a typical comparison of TGA curves between N_2 and CO_2 atmospheres (Fig. 3), CO_2 assisted in the pyrolysis of ovalbumin and therefore the protein in algae, which shows a more significant weight loss rate compared with that under N_2. However, the weight loss curves of cellulose and oil droplet pyrolysis derived in CO_2 stayed consistent with curves under N_2. This refers to the findings that CO_2 does not participate in the pyrolysis of carbohydrate and lipid contained in algae.

3.2. Kinetic study

3.2.1. Determination of activation energy via Kissinger- Akahira-Sunose (KAS)

Amongst the three stages of pyrolysis, the second stage-devolatilization is regarded as the main step in algae decomposition, and thus the main scope of this study. Based on the starting and finishing temperatures, under both atmospheres, ovalbumin was the first to decompose at around 180 °C and sustained until 600 °C at which the weight loss rate was nearly zero. Cellulose was the second to pyrolyze at about 250–500 °C and oil droplet was the last to initiate its pyrolysis at 300 °C and finishing at around 550 °C. As a result of the synergistic effect of protein, carbohydrate and lipid in algae, the actual spirulina decomposed within a smaller temperature range, but still within the decomposition range of the

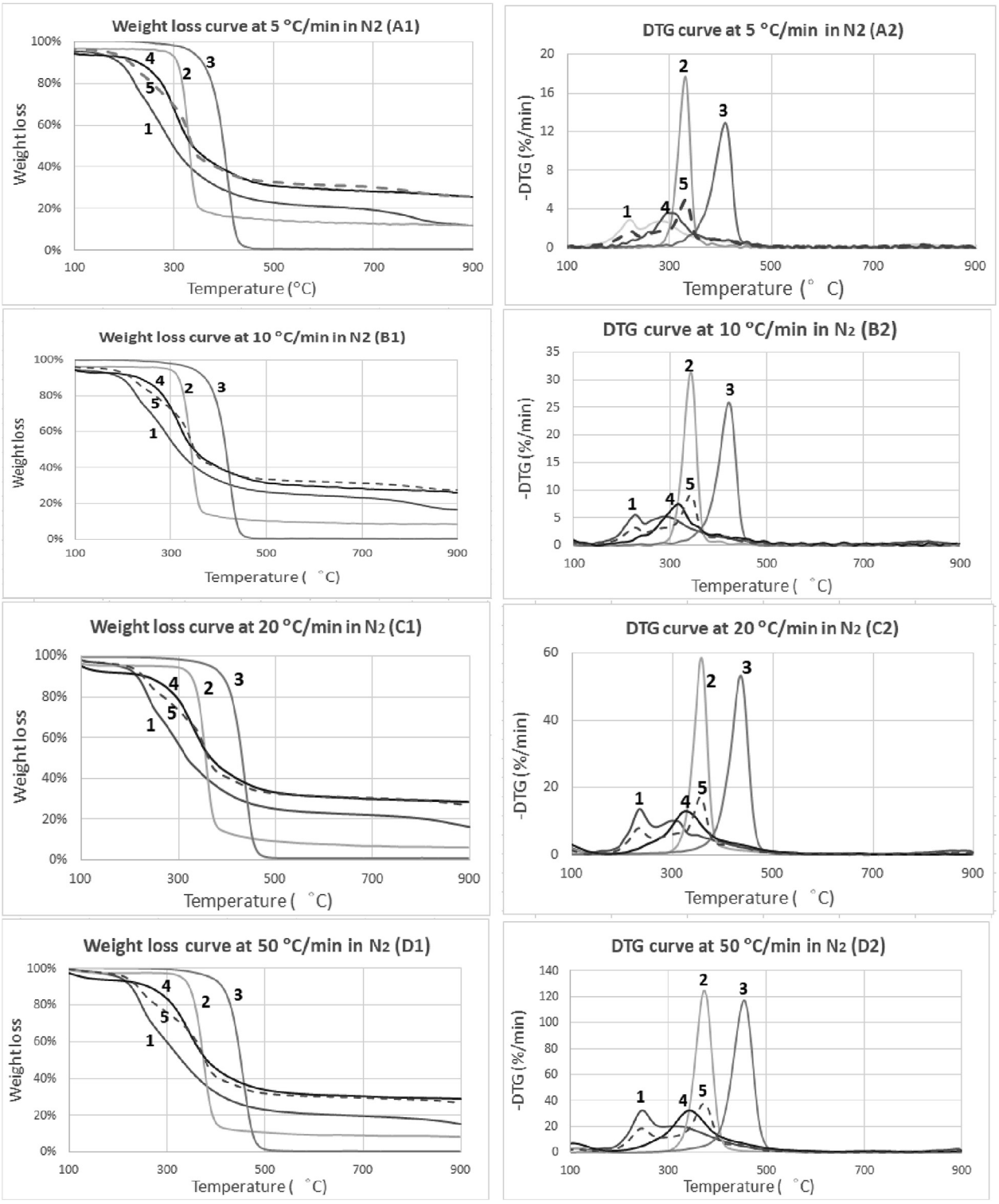

Fig. 1. TG (1) and DTG (2) curves of the pyrolysis of ovalbumin (1), cellulose (2), oil droplet (3), spirulina (4) and simulative spirulina (5) under N_2 at different heating rates of 5 (A), 10 (B), 20 (C), and 50 (D) °C/min.

three individual components, at around 220 °C and terminating at 420 °C. Therefore, after considering the pyrolysis of all four samples, the temperature range for applying KAS method was selected as 120–600 °C, which covered the temperatures of the whole conversion process.

To study the dependence of activation energy of model compounds on the increasing conversion rate (α), 19 different conversion rates from 5% to 95% at 5% intervals were investigated at four heating rates of 5, 10, 20 and 50 °C/min under N_2 and CO_2 based on KAS method. The activation energy (E_a) and correlation factor (R^2) of model compounds are listed in Table A in the supplementary material and summarized as Fig. 4. Generally, due to

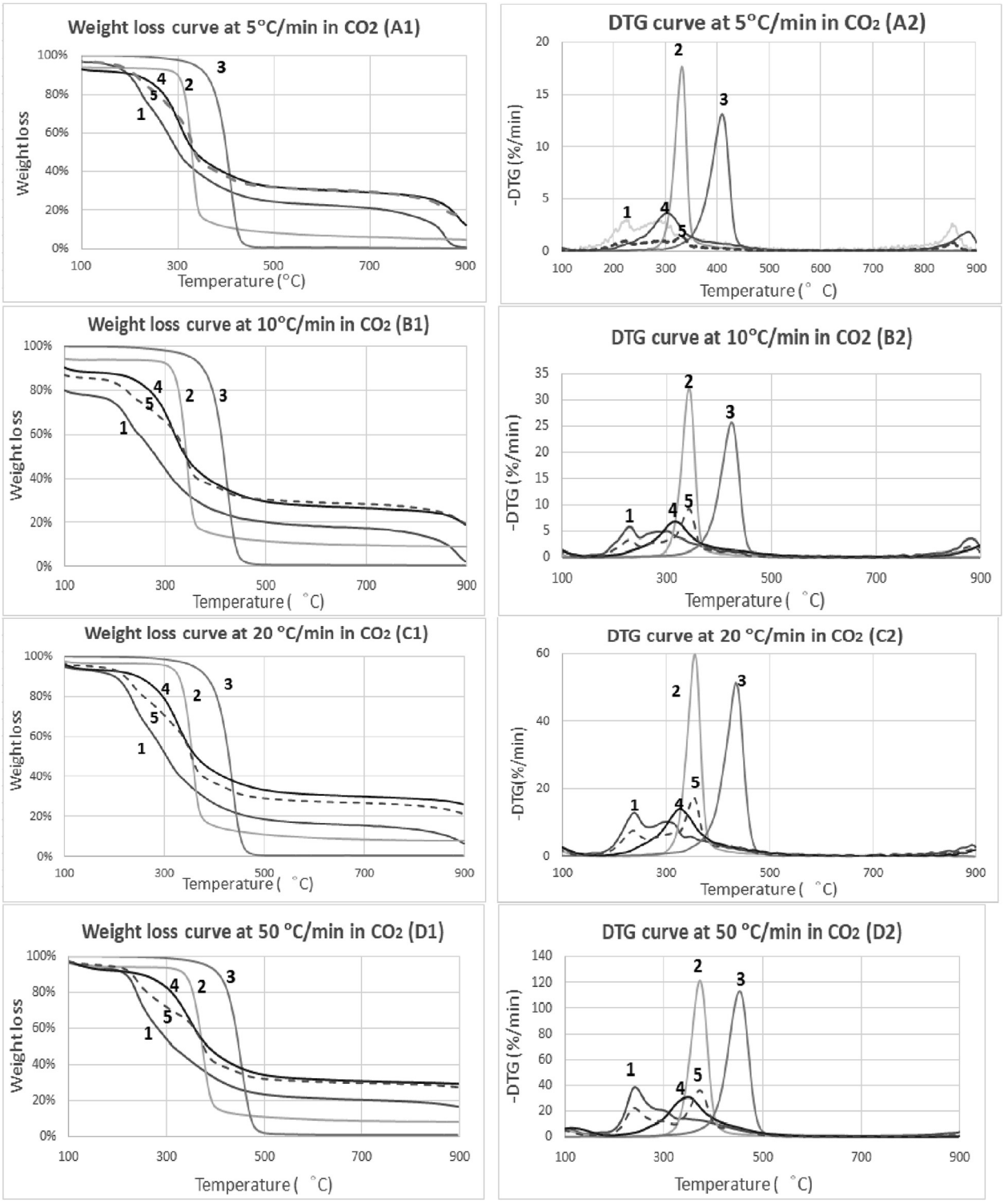

Fig. 2. TG (1) and DTG (2) curves of the pyrolysis of ovalbumin (1), cellulose (2), oil droplet (3), spirulina (4) and simulative spirulina (5) under CO_2 at different heating rates of 5 (A), 10 (B), 20 (C), and 50 (D) °C/min.

the delay of heat transfer from pan to sample, the thermal lag was inherited into the process as the evidence from the shift of DTG peak values towards higher temperature zone as the heating rate increased. The activation energy derived, via KAS method, during the main stage of pyrolysis is of sufficient accuracy and can be deployed for analysis [38]. Moreover, the R^2 values derived for this stage are mostly above 0.90, which indicates the reliability of the calculated E_a. However, the initial and final stages of sample conversion might contain unavoidable errors due to the compositional heterogeneity of solid sample and experimental errors [39,40]. Fig. 4 shows the plot of activation energy obtained from KAS method against the conversion rate under N_2 and CO_2 atmosphere

Table 2
Features of the pyrolysis of cellulose, ovalbumin, oil droplet and spirulina under N_2 and CO_2.

Sample		N_2				CO_2			
	β (°C min^{-1})	5	10	20	50	5	10	20	50
Ovalbumin	Y_{char} (%)	14.4	20.2	20.2	18.4	15.9	14.6	14.0	19.5
	T_i (°C)	186	193	197	208	187	197	202	214
	T_m (°C)	219	228	232	242	216	224	231	245
	D_m (%/min)	−2.3	−4.7	−9.7	−23.9	−2.3	−4.4	−9.0	−25.1
	$\Delta T_{1/2}$ (°C)	78	92	123	137	87	93	98	140
Cellulose	Y_{char} (%)	12.1	8.6	6.6	8.8	5.4	9.3	8.1	8.7
	T_i (°C)	299	309	319	330	297	289	318	330
	T_m (°C)	326	338	349	364	325	338	350	364
	D_m (%/min)	−13.6	−25.2	−47.4	−100.1	−13.9	−25.5	−47.8	−101.5
	$\Delta T_{1/2}$ (°C)	67	85	125	176	67	81	90	143
Oil droplet	Y_{char} (%)	0.5	0.5	0.7	0.7	0.4	0.6	0.7	0.9
	T_i (°C)	240	255	261	274	209	223	226	233
	T_m (°C)	410	422	437	455	410	423	435	449
	D_m (%/min)	−13.5	−25.9	−53.0	−114.2	−13.1	−25.7	−51.4	−115.0
	$\Delta T_{1/2}$ (°C)	91	106	114	135	108	119	115	107
Spirulina	Y_{char} (%)	27.0	27.0	29.2	29.6	27.0	25.5	28.7	30.1
	T_i (°C)	225	235	243	255	227	236	243	254
	T_m (°C)	300	310	322	338	296	306	322	337
	D_m (%/min)	−2.9	−5.8	−11.5	−27.6	−2.8	−5.8	−10.9	−24.8
	$\Delta T_{1/2}$ (°C)	125	146	169	192	131	143	178	194

* Y_{char} is the weight percentage of char residue at 800 °C; T_i is the initial temperature when volatile matters start to release; D_m is the maximum weight loss rate; T_m is the peak temperature; $\Delta T_{1/2}$ is the half peak width temperature.

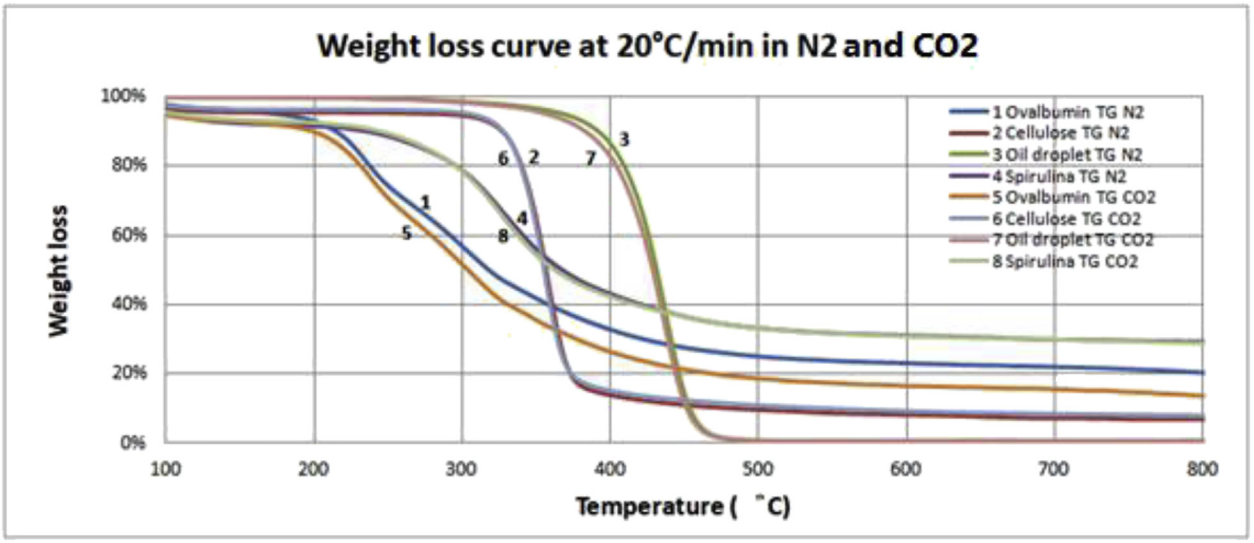

Fig. 3. wt loss curves of ovalbumin (1 and 5), cellulose (2 and6), oil droplet (3 and 7) and spirulina (4 and 8) at 20 °C/min in N_2 and CO_2.

for the pyrolysis of model compounds and actual algae.

It is noticed that E_a of three model compounds varied along with the increment of conversion rate. The E_a of oil droplet increased gradually from 123.1 to 175.2 kJ/mol within the conversion range of 5–45%, after which it remained relatively unchanged starting from around 180 kJ/mol in N_2. Similarly, when CO_2 was used, E_a of oil droplet progressively increased from 156.9 to 197.3 kJ/mol within the conversion rate of 5–45%, while that value fluctuated at about 200 kJ/mol from 50 to 95% conversion. The E_a values were 5.3–27.5% larger than those derived in N_2, which suggested that the lipid content in algae is relatively more stable and difficult to decompose under CO_2 atmosphere. The results agreed with the initial test at the beginning of pyrolysis where oil droplet showed the highest activation energy amongst the three model compounds, which was corresponding to the order of T_i values in TG analysis.

A contrary trend was found in the pyrolysis of cellulose under N_2 atmosphere, where the activation energy reduced gradually from 202.5 to 171.4 kJ/mol for the conversion of 5–90%. As for the pyrolysis of cellulose in CO_2, the activation energy also decreased from 187.6 to 171.5 kJ/mol for the same conversion range. According to Fig. 4, a slightly lower activation energy was recorded for the decomposition of cellulose under CO_2, in comparison with the energy calculated using N_2 as the carrier gas. This is in opposition to what was found in the pyrolysis of lipid.

As for the ovalbumin, the activation energy increased from 188.4 to 209.9 kJ/mol when the conversion (α) increased from 5 to 20%. It increased slightly to 230 kJ/mol when the conversion increased to 55% and peaked at 331.6 kJ/mol when conversion was 75%. E_a values could be ignored beyond the conversion rate of 80%, which is due to the crossover of TG weight loss curve resulted from the heterogeneous nature of the composition of solid samples [41]. However,

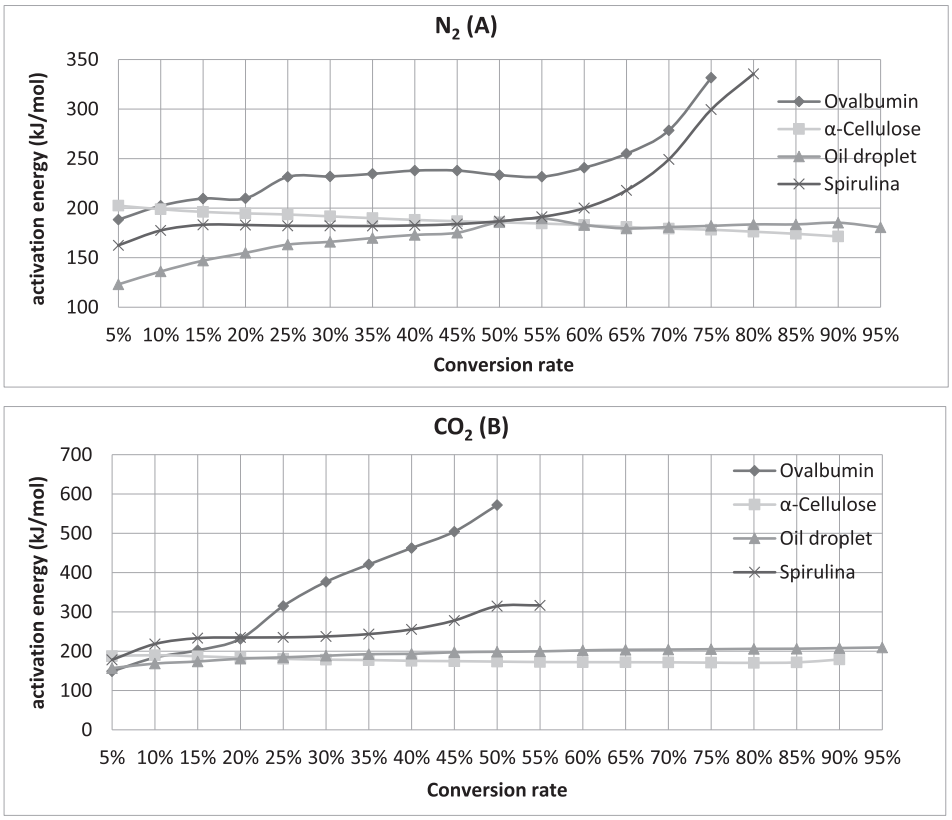

Fig. 4. The activation energy of ovalbumin, cellulose, oil droplet and spirulina against the conversion rate under N_2 (A) and CO_2 (B).

the activation energy distribution indicated a different pattern in CO_2. The energy required increased significantly from 148.9 to 572 kJ/mol for the conversion range of 5%–50%. After that, the activation energy declined to lower than zero. The exhaustion of ovalbumin occurred after the conversion rate of 55%. This indicates that the pyrolysis of ovalbumin under CO_2 is more feasible at conversion rate lower than 30%, and the whole process is more efficient compared with N_2 as the carrier gas.

For the pyrolysis of spirulina under N_2, the activation energy increased from 160 to 180 kJ/mol ($5\% < \alpha < 15\%$) and increased steadily to 190 kJ/mol ($20\% < \alpha < 50\%$), after which the value surged to 335 kJ/mol ($55\% < \alpha < 80\%$). Similar to the pyrolysis of ovalbumin, the activation energy decreased dramatically to nearly zero. Since a large proportion of spirulina consists of protein with a content of 57.8 wt %, the activation energy for the pyrolysis of this algae followed a similar trend, as shown in ovalbumin under CO_2. This is concluded from the increase in E_a during the initial stage from 178 to 317 kJ/mol ($5\% < \alpha < 55\%$). It is also obvious that the pyrolysis in CO_2 required higher activation energy compared to N_2 as the carrier gas, but the pyrolysis in CO_2 proceeded quicker and ended earlier.

Overall, by comparing activation energy derived from the pyrolysis of three model compounds under N_2 and CO_2, the ovalbumin required a lower amount of energy to decompose, and the process proceeded quicker under CO_2 atmosphere. It was found in this study that CO_2 could assist in the pyrolysis of algal protein. Proteins are long chains of polymerized amino acids, also involved in cell structure. There are various species of protein contained in algae since one single cell produces thousands of different proteins with different amino acid composition. The nitrogen-released compounds are mainly in the form of organic nitrites, nitriles, amines, amides, indoles, pyrroles and their derivatives [42].

However, under CO_2 atmosphere, the activation energy remained relatively unchanged for the pyrolysis of cellulose, while higher activation energy of oil droplet highlighted the difficulty for algal lipid to decompose.

3.2.2. Determination of reaction model via Coats- Redfern method

According to TG/DTG analysis, heating rate affected the pyrolysis process significantly. Due to the severe thermal lag, the kinetic factors calculated based on high heating rates were usually underestimated values as compared to the actual values [43,44]. The total time for pyrolysis would be reduced by the rising heating rate, so is the period of heat transfer from pan to the sample; thus, the temperature of decomposition will be drifted to higher temperatures. Hence, to minimize the influence of thermal hysteresis, the result collected under low pyrolysis heating rate of 5 °C/min was used to determine the reaction model. A similar approach was carried out in other open literature [8,10]. Commonly-used mechanism models were substituted into Coats-Redfern method to plot $ln\frac{G(\alpha)}{T^2}$ against $-\frac{1}{RT}$ for the main pyrolysis stage. As the temperature increases, the degradation of samples could be divided into two ranges (Events I and II) under different reaction mechanisms. On the basis of R^2 fitting method, the category of mechanism, activation energy (E_a), and pre-exponential (A) corresponding to the best regression value, among the application of each form, $G(\alpha)$, as shown in Table 3.

According to Fig. 4, the activation energy of ovalbumin would increase gradually during the initial decomposition stage and rocket to high values in the end, which indicated that the two-reaction mechanism dominated this stage of pyrolysis. The carbonaceous matters of ovalbumin were the first to decompose from 180 °C, which fitted well with the Second-order chemical reaction (F2) model, and required the lowest activation energy of 74.4 kJ/mol. As the pyrolysis temperature increased, the activation energy

Table 3
Activation energy, pre-exponential factor and related kinetic models of Events I and II under N_2 and CO_2.

		N_2				CO_2			
	Parameters	Ovalbumin	Cellulose	Oil droplet	Spirulina	Ovalbumin	Cellulose	Oil droplet	Spirulina
Event I	**Range(°C)**	180–220	300–325	340–440	220–270	180–220	300–325	340–430	220–300
	E_a (kJ/mol)	74.4	273.0	227.8	121.7	66.8	266.6	266.5	20.7
	Mechanism	Second-order reaction (F2)	First-order reaction (F1)	1-D diffusion (D1)	1-D diffusion (D1)	Second-order reaction (F2)	First-order reaction (F1)	2-D diffusion (D2)	1-D diffusion (D1)
	A (s^{-1})	3.3×10^6	23.4	1.4×10^{16}	4.6×10^4	4.0×10^5	22.8	2.29×10^{19}	0.3
Event II	**Range(°C)**	220–400	325–350		270–380	220–400	325–350		300–360
	E_a (kJ/mol)	41.5	377.4		53.0	24.4	344.2		62.1
	Mechanism	Second-order reaction (F2)	Second-order reaction (F2)		Second-order reaction (F2)	Second-order reaction (F2)	Second-order reaction (F2)		Second-order reaction (F2)
	A (s^{-1})	164.7	32.8		4.3×10^9	0.6	29.9		4.5

of ovalbumin in Event II reduced to 41.5 kJ/mol from 220 °C, which was much lower than the value derived by KAS method, and the mechanism of ovalbumin pyrolysis remained as F2 model. Cellulose was the second model compound to decompose from 300 to 360 °C, which required higher activation energy of the First-order chemical reaction (F1) model (273.0 kJ/mol) in the temperature range of 300–325 °C, followed by Event II. From 325 to 350 °C, the E_a increased to 377.4 kJ/mol in F2 model. Compared to the results concluded from the KAS method, the activation energy is very different. The E_a decreased from 202.5 to 171.4 kJ/mol during the whole period of pyrolysis and increased to about 198.4 kJ/mol at $\alpha = 0.95$. Similarly, oil droplet did not alter evidently and therefore, one reaction model was used in the pyrolysis process, which appeared to be 1-D diffusion (D1) model. It was the last model substance to decompose at 340 °C until 440 °C with an activation energy of 227.8 kJ/mol, which was higher than the value obtained via KAS method (approximately 180 kJ/mol). Hence, the protein in algae was the first primary component to decompose during the second stage, followed by carbohydrate which has higher activation energy whilst protein continued to generate volatiles. Lipid in algae was the last component to pyrolyze, which required higher activation energy and decomposed with the remaining carbohydrate and protein, simultaneously. However, the decomposition of spirulina was found to be in D1 model with an activation energy of 122.6 kJ/mol from 220 to 270 °C. After 270 °C, the mechanism was changed to F2 model and the E_a required was reduced to an amount of 53.0 kJ/mol.

As for the CO_2 atmosphere, ovalbumin was the first sample to decompose in F2 mechanism which is the same as the decomposition under N_2 with only 66.8 kJ/mol activation energy from 180 °C. After 220 °C. The activation energy then followed the same decreasing trend in F2 model to 24.4 kJ/mol as N_2 atmosphere. Meanwhile, compared with N_2 atmosphere, cellulose started to decompose in F1 model from 300 to 325 °C with similar activation energy (266.6 kJ/mol) and pre-exponential factor (22.8). The E_a further increased to 344.2 kJ/mol in the temperature range of 325–350 °C in F2 model, which is comparable to the parameters derived under N_2. On the other hand, the oil droplet decomposed with a higher activation energy of 266.5 kJ/mol, compared to the value under the N_2 atmosphere. Therefore, it is evident that a similar decomposition sequence of the three model compounds can be observed under CO_2, compared to N_2 as the carrier gas. Moreover, the activation energy for the decomposition of the ovalbumin is smaller, which suggests that ovalbumin is easier to decompose in the CO_2 atmosphere. As for the lipid, its decomposition occurred at higher temperature with lower degradation rate and higher activation energy, which suggests that it is difficult to decompose in CO_2 atmosphere. This leads to the same conclusion as using KAS method. Spirulina required less energy to proceed the decomposition under CO_2, which decomposed in D1 model with 20.7 kJ/mol for Event I, and switched to F2 mechanism with E_a of 36.4 kJ/mol, compared to the decomposition under N_2 atmosphere.

The Coats-Redfern method, which is commonly applied in the determination of reaction mechanism of biomass pyrolysis [45], requires the use of only one set of TG data, while iso-conversional method (KAS) needs at least three sets of data to calculate the thermal parameters. However, different methods are not exclusive, but mutually complementary in the analysis of reaction mechanism [46].

3.3. Characteristics of char

Table 4 summarizes the composition of char remaining after pyrolysis under N_2 and CO_2 in four different heating rates. As there was minimal char left in the crucibles after pyrolysis of oil droplet (<1 wt%), hence, there are no results for char of algal pseudo-lipid. The compositions of ovalbumin char changed significantly after pyrolysis under N_2 when four different heating rates were used. Carbon and oxygen content of the char fluctuated around 25 and 70 wt %, respectively. But after pyrolysis in CO_2, the carbon content increased with the increasing of heating rate which then became similar at higher heating rates of 20 and 50 °C/min (14.9–22.2 wt%). This was also observed for the oxygen content (55.9–67.6 wt%). It is apparent that using CO_2 as carrier gas could reduce the carbon and oxygen content in ovalbumin char residue as well as the overall char amount. This reconfirms the previous findings where a smaller activation energy is required for the pyrolysis of ovalbumin in CO_2 as reported in Section 3.2.1. Due to the longer processing time required for lower heating rates (170 min for 5 °C/min, 85 min for 10 °C/min, 42.5 min for 20 °C/min and 17 min for 50 °C/min), the sample had sufficient time to contact and react with CO_2 via $C + CO_2 \rightarrow 2CO$ reaction. This reduced the carbon content in char significantly, while increasing the compositions of other elements. Elements including Na, Mg, Si, P, K, and Ca, in the char of ovalbumin pyrolyzed under CO_2 increased steadily as the heating rate was reduced. At the heating rate of 5 °C/min, these elements were significantly larger than the amount derived under N_2, especially for P, K, Ca, and Mg at 8.0, 10.3, 1.6 and 2.1 wt %, respectively.

As for the cellulose, the elements in char remained relatively the same for both N_2 and CO_2 atmospheres even in various heating rates (carbon, 27.3 wt%; oxygen, 72.7 wt%). This also corresponded to the relatively unchanged activation energy calculated in Section 3.2.1. This also indicated that CO_2 minimally participated in the pyrolysis of carbohydrate contained in algae.

Similar to the composition of ovalbumin char, C and O content of spirulina char under four heating rates varied around 25 and 70 wt % in N_2. However, char derived in CO_2 contained an increased amount of carbon and oxygen as the heating rates became larger

Table 4
Elemental compositions of solid residues of ovalbumin, cellulose and spirulina derived by EDS.

Ovalbumin												
Heating rate (°C/min)	N_2				CO_2				Char (CO_2)			
	5	10	20	50	5	10	20	50	5	10	20	50
C	25.4	25.6	25.6	25.5	14.9	20.0	22.2	22.2	15.1	28.6	29.6	29.0
N	–	–	0.4	0.3	–	0.9	0.9	1.7	–	–	–	–
Na	–	–	–	–	0.3	–	–	–	9.5	7.2	5.7	5.3
Mg	0.4	0.4	0.4	0.3	2.1	0.9	0.5	0.4	6.3	6.8	4.4	4.5
Si	–	–	–	–	0.1	–	–	–	–	0.1	0.1	–
P	1.4	1.2	1.2	1.0	8.0	2.8	2.2	1.5	13.2	11.9	9.6	11.6
S	–	–	–	0.1	–	–	–	–	–	–	–	–
Cl	–	–	–	–	–	0.1	–	–	–	–	–	–
K	2.2	2.1	1.8	1.4	10.3	4.5	3.6	1.8	0.3	0.4	0.4	0.6
Ca	0.4	0.2	0.2	0.2	1.6	0.4	0.7	0.2	11.6	11.9	12.9	16.5
Fe	–	–	–	0.1	–	–	–	–	0.2	0.6	0.2	0.3
O	70.3	70.5	70.6	70.8	55.9	62.9	66.4	67.6	43.0	31.8	36.6	31.6
Cellulose												
Heating rate (°C/min)	N_2				CO_2				Char (CO_2)			
	5	10	20	50	5	10	20	50	5	10	20	50
C	27.3	27.3	27.3	27.3	27.3	27.3	27.3	27.3	92.9	90.5	94.3	94.0
O	72.7	72.7	72.7	72.7	72.7	72.7	72.7	72.7	7.1	9.5	5.7	6.0
Spirulina												
Heating rate (°C/min)	N_2				CO_2				Char (CO_2)			
	5	10	20	50	5	10	20	50	5	10	20	50
C	25.4	23.1	24.1	25.0	3.7	15.2	23.8	24.5	2.0	7.7	9.2	9.1
N	–	–	0.7	0.8	–	–	–	–	–	–	–	–
Na	0.4	0.5	0.6	0.4	2.5	1.7	0.8	0.7	4.7	2.6	4.3	2.9
Mg	0.5	0.8	0.6	0.4	4.5	2.3	0.8	0.7	5.9	6.8	4.8	4.9
Al	0.1	0.3	0.3	0.2	3.0	0.9	0.6	0.1	2.2	1.8	2.9	3.1
Si	0.4	0.4	0.2	0.2	2.8	1.0	0.9	0.3	5.2	2.5	5.4	4.1
P	1.4	2.5	1.2	0.9	14.9	5.9	1.8	1.3	13.1	12.1	11.2	11.6
S	0.1	0.1	–	–	–	0.1	0.1	–	–	0.1	–	–
Cl	–	–	–	–	–	0.1	–	–	0.1	–	–	–
K	0.9	1.5	1.0	0.8	13.7	7.0	1.8	1.6	9.4	9.7	7.7	10.3
Ca	0.3	2.1	0.7	0.2	3.4	2.0	0.8	0.4	5.2	10.4	4.2	6.7
Fe	0.1	1.0	0.3	0.4	3.6	1.8	1.1	0.4	4.2	5.6	3.0	4.3
O	70.8	67.8	70.2	70.9	45.2	56.3	68.0	69.8	47.7	34.4	47.3	42.8

from 5 to 50 °C/min (3.7–24.5 wt% and 45.2 to 69.8 wt % respectively). At a heating rate of 5 °C/min, elements of char obtained in CO_2, including P, K, Na, Mg, Al, Si, Ca, and Fe were significantly larger than the amount derived in N_2, especially for P and K with 14.9 and 13.7 wt %, respectively.

The different heating rates have significant influences on the carbon content in char. Overwhelming CO_2 reacted significantly with carbon content in char, which improves the cracking of VOCs in proteins of algae. The reaction between VOCs and CO_2 helped to reduce hydrocarbons, such as tar [47]. The specific reaction between VOCs and CO_2 would be further investigated after the TGA coupled with a GC-MS as TG/GC-MS. The carbon content will increase with the increment of heating rate. In order to investigate the effects of processing time on the carbon content of solid residue, the pyrolysis of char which was carried out in the tube furnace (using a simulated TGA process at 5 °C/min) was conducted under four heating rates in CO_2 atmosphere. As the heating rate increased from 5 to 50 °C/min, the carbon content of cellulose char remained steady at around 93 wt %, which suggested that CO_2 minimally affected the pyrolysis of algal carbohydrate. On the other hand, the carbon content of the newly-prepared char from ovalbumin increased from 15.1 to 29.0 wt %. This indicated that CO_2 atmosphere would participate in the reaction with carbon contained in char as the pyrolysis progressed, mainly due to the gasification of CO_2 and carbon content.

4. Conclusions

Pyrolysis characteristics of three algal model compounds (cellulose, ovalbumin, oil droplet) and algae (spirulina) were investigated by TGA and analysed using model-free (KAS) and model fitting (Coats-Redfern) methods. It was found that pyrolysis was more efficient at lower heating rates. The algal protein was the first to decompose with the lowest activated energy, followed by carbohydrate and lipid contained in algae. Moreover, CO_2 atmosphere favored the pyrolysis of protein due to the improved cracking of VOCs in ovalbumin as well as the reaction between VOCs and CO_2. However, the decomposition of lipid and carbohydrate was less feasible in CO_2 atmosphere.

Acknowledgement

Ministry of Science and Technology of China(National Key R&D Programme, 2017YFB0602601] and the Natural Science Foundation of China (5160060426) are acknowledged for their financial support to this study. The International Doctoral Innovation Centre is also acknowledged for the provision of a full scholarship to the first author. Dr Yu Hong is currently working for the R&D Centre, Ningbo Thermal Power Co. Ltd.

Appendix A. Supplementary data

Supplementary data to this article can be found online at https://doi.org/10.1016/j.renene.2019.07.135.

References

[1] J. Yan, K. Shi, C. Pang, E. Lester, T. Wu, Influence of minerals on the thermal processing of bamboo with a suite of carbonaceous materials, Fuel 180 (2016)

256–262.
[2] R. Zhang, L. Li, D. Tong, C. Hu, Microwave-enhanced pyrolysis of natural algae from water blooms, Bioresour. Technol. 212 (2016) 311–317.
[3] Q. Xie, M. Addy, S. Liu, B. Zhang, Y. Cheng, Y. Wan, Y. Li, Y. Liu, X. Lin, P. Chen, R. Ruan, Fast microwave-assisted catalytic co-pyrolysis of microalgae and scum for bio-oil production, Fuel 160 (2015) 577–582.
[4] D. Beneroso, J.M. Bermudez, A. Arenillas, J.A. Menendez, Microwave pyrolysis of microalgae for high syngas production, Bioresour. Technol. 144 (2013) 240–246.
[5] L. Rodolfi, G. Zittelli, N. Bassi, G. Padovani, N. Biondi, G. Bonini, M. Tredici, Microalgae for oil: strain selection, induction of lipid synthesis and outdoor mass cultivation in a low-cost photobioreactor, Biotechnol. Bioeng. 102 (1) (2009) 100–112.
[6] Y. Hong, W. Chen, X. Luo, C. Pang, E. Lester, T. Wu, Microwave-enhanced pyrolysis of macroalgae and microalgae for syngas production, Bioresour. Technol. 237 (2017) 47–56.
[7] R. Sharma, P.N. Sheth, A.M. Gujrathi, Kinetic modeling and simulation: pyrolysis of Jatropha residue de-oiled cake, Renew. Energy 86 (2016) 554–562.
[8] S. Wang, H. Lin, B. Ru, G. Dai, X. Wang, G. Xiao, Z. Luo, Kinetic modeling of biomass components pyrolysis using a sequential and coupling method, Fuel 185 (2016) 763–771.
[9] A. Zaker, Z. Chen, X. Wang, Q. Zhang, Microwave-assisted pyrolysis of sewage sludge: a review, Fuel Process. Technol. 187 (2019) 84–104.
[10] R. Maurya, T. Ghosh, H. Saravaia, C. Paliwal, A. Ghosh, S. Mishra, Non-isothermal pyrolysis of de-oiled microalgal biomass: kinetics and evolved gas analysis, Bioresour. Technol. 221 (2016) 251–261.
[11] S. Vyazovkin, A unified approach to kinetic processing of nonisothermal data, Int. J. Chem. Kinet. 28 (2) (1996) 95–101.
[12] M. Hu, X. Wang, J. Chen, P. Yang, C. Liu, B. Xiao, D. Guo, Kinetic study and syngas production from pyrolysis of forestry waste, Energy Convers. Manag. 135 (2017) 453–462.
[13] S. Vyazovkin, A.K. Burnham, J.M. Criado, L.A. Pérez-Maqueda, C. Popescu, N. Sbirrazzuoli, ICTAC Kinetics Committee recommendations for performing kinetic computations on thermal analysis data, Thermochim. Acta 520 (1–2) (2011) 1–19.
[14] S. Ceylan, D. Kazan, Pyrolysis kinetics and thermal characteristics of microalgae Nannochloropsis oculata and Tetraselmis sp, Bioresour. Technol. 187 (2015) 1–5.
[15] S. Ceylan, Y. Topcu, Z. Ceylan, Thermal behaviour and kinetics of alga Polysiphonia elongata biomass during pyrolysis, Bioresour. Technol. 171 (1) (2014) 193–198.
[16] C. Gai, Y. Zhang, W.T. Chen, P. Zhang, Y. Dong, Thermogravimetric and kinetic analysis of thermal decomposition characteristics of low-lipid microalgae, Bioresour. Technol. 150 (3) (2013) 139–148.
[17] J. Lee, J.-I. Oh, Y.S. Ok, E.E. Kwon, Study on susceptibility of CO2-assisted pyrolysis of various biomass to CO2, Energy 137 (2017) 510–517.
[18] L. Tang, Y. Yan, Y. Meng, J. Wang, P. Jiang, C.H. Pang, T. Wu, CO2 gasification and pyrolysis reactivity evaluation of oil shale, Energy Procedia 158 (2019) 1694–1699.
[19] L. Li, R. Zhang, D. Tong, C. Hu, Fractional pyrolysis of algae and model compounds†, Chin. J. Chem. Phys. 28 (4) (2015) 525–532.
[20] M.T. Cesário, M.M.R. da Fonseca, M.M. Marques, M.C.M.D. de Almeida, Marine algal carbohydrates as carbon sources for the production of biochemicals and biomaterials, Biotechnol. Adv. 36 (3) (2018) 798–817.
[21] L. Sheng, X. Wang, X. Yang, Prediction model of biocrude yield and nitrogen heterocyclic compounds analysis by hydrothermal liquefaction of microalgae with model compounds, Bioresour. Technol. 247 (2018) 14–20.
[22] T. Wu, M. Gong, E. Lester, F. Wang, Z. Zhou, Z. Yu, Characterisation of residual carbon from entrained-bed coal water slurry gasifiers, Fuel 86 (7–8) (2007) 972–982.
[23] J. Oladejo, S. Adegbite, X. Gao, H. Liu, T. Wu, Catalytic and non-catalytic synergistic effects and their individual contributions to improved combustion performance of coal/biomass blends, Appl. Energy 211 (2018) 334–345.
[24] A.M. Parvez, T. Wu, Characteristics and interactions between coal and carbonaceous wastes during co-combustion, J. Energy Inst. 90 (1) (2017) 12–20.
[25] A.M. Parvez, Y. Hong, E. Lester, T. Wu, Enhancing the reactivity of petroleum coke in CO2 via Co-processing with selected carbonaceous materials, Energy Fuels 31 (2) (2017) 1555–1563.
[26] A.C.R. Lim, B.L.F. Chin, Z.A. Jawad, K.L. Hii, Kinetic analysis of rice husk pyrolysis using kissinger-akahira-sunose (KAS) method ☆, Procedia Eng. 148 (2016) 1247–1251.
[27] I. Ali, S.R. Naqvi, A. Bahadar, Kinetic analysis of Botryococcus braunii pyrolysis using model-free and model fitting methods, Fuel 214 (2018) 369–380.
[28] L. Tian, A. Tahmasebi, J. Yu, An experimental study on thermal decomposition behavior of magnesite, J. Therm. Anal. Calorim. 118 (3) (2014) 1577–1584.
[29] S.Y. Yorulmaz, A.T. Atimtay, Investigation of combustion kinetics of treated and untreated waste wood samples with thermogravimetric analysis, Fuel Process. Technol. 90 (7–8) (2009) 939–946.
[30] Q.V. Bach, W.H. Chen, A comprehensive study on pyrolysis kinetics of microalgal biomass, Energy Convers. Manag. 131 (2017) 109–116.
[31] W.P. Chan, J.-Y. Wang, Characterisation of sludge for pyrolysis conversion process based on biomass composition analysis and simulation of pyrolytic properties, Waste Manag. 72 (2018) 274–286.
[32] W.P. Chan, J.-Y. Wang, Formation of synthetic sludge as a representative tool for thermochemical conversion modelling and performance analysis of sewage sludge – based on a TG-FTIR study, J. Anal. Appl. Pyrolysis 133 (2018) 97–106.
[33] S.R. Naqvi, R. Tariq, Z. Hameed, I. Ali, M. Naqvi, W.-H. Chen, S. Ceylan, H. Rashid, J. Ahmad, S.A. Taqvi, M. Shahbaz, Pyrolysis of high ash sewage sludge: kinetics and thermodynamic analysis using Coats-Redfern method, Renew. Energy 131 (2019) 854–860.
[34] A. Plis, J. Lasek, A. Skawińska, J. Zuwała, Thermochemical and kinetic analysis of the pyrolysis process in Cladophora glomerata algae, J. Anal. Appl. Pyrolysis 115 (2015) 166–174.
[35] P. Giudicianni, G. Cardone, R. Ragucci, Cellulose, hemicellulose and lignin slow steam pyrolysis: thermal decomposition of biomass components mixtures, J. Anal. Appl. Pyrolysis 100 (2013) 213–222.
[36] X. Dai, C. Wu, L. Haibin, Y. Chen, The fast pyrolysis of biomass in CFB reactor, Energy Fuels 14 (3) (2000) 552–557.
[37] R. Comesaña, M.A. Gómez, M.A. Álvarez, P. Eguía, Thermal lag analysis on a simulated TGA-DSC device, Thermochim. Acta 547 (2012) 13–21.
[38] A.I. Casoni, J. Zunino, M.C. Piccolo, M.A. Volpe, Valorization of Rhizoclonium sp. algae via pyrolysis and catalytic pyrolysis, Bioresour. Technol. 216 (2016) 302–307.
[39] N. Sbirrazzuoli, L. Vincent, A. Mija, N. Guigo, Integral, differential and advanced isoconversional methods : complex mechanisms and isothermal predicted conversion–time curves, Chemometr. Intell. Lab. Syst. 96 (2) (2009) 219–226.
[40] W.P. Chan, J.Y. Wang, Comparison study on thermal degradation behaviours and product distributions for various types of sludge by using TG-FTIR and fixed bed pyrolysis, J. Anal. Appl. Pyrolysis 121 (2016) 177–189.
[41] D.L. Urban, M.J.A. Jr, Study of the kinetics of sewage sludge pyrolysis using DSC and TGA, Fuel 61 (9) (1982) 799–806.
[42] P.E. Amaral Debiagi, M. Trinchera, A. Frassoldati, T. Faravelli, R. Vinu, E. Ranzi, Algae characterization and multistep pyrolysis mechanism, J. Anal. Appl. Pyrolysis 128 (2017) 423–436.
[43] R.N. And, M.J. Antal, Thermal lag, fusion, and the compensation effect during biomass pyrolysis†, Ind. Eng. Chem. Res. 35 (5) (1996) 1711–1721.
[44] M. Grønli, M.J. Antal, G. Várhegyi, A round-robin study of cellulose pyrolysis kinetics by thermogravimetry, Ind. Eng. Chem. Res. 38 (6) (1999) 2238–2244.
[45] W. Gao, K. Chen, J. Zeng, J. Xu, B. Wang, Thermal pyrolysis characteristics of macroalgae Cladophora glomerata, Bioresour. Technol. 243 (2017) 212–217.
[46] S. Feng, P. Li, Z. Liu, Y. Zhang, Z. Li, Experimentsal study on pyrolysis characteristic of coking coal from Ningdong coalfield, J. Energy Inst. 91 (2) (2018) 233–239.
[47] J. Kim, K.-H. Kim, E.E. Kwon, Enhanced thermal cracking of VOCs evolved from the thermal degradation of lignin using CO2, Energy 100 (2016) 51–57.